Title: Development and clinical validation of a targeted RNAseq panel (Fusion-STAMP) for diagnostic and predictive gene fusion detection in solid tumors

Short Title: FFPE fusion detection by RNAseq

Authors: Erik Nohr[1,2], Christian A. Kunder[1,2], Carol Jones[2], Shirley Sutton[3], Eula Fung[2], Hongbo Zhu[2], Sharon J. Feng[1], Linda Gojenola[2], Carlos D. Bustamante[3,4], James L. Zehnder[1,2], Helio A. Costa[1,2,4*]

Affiliations:
[1]Department of Pathology, Stanford University School of Medicine, Stanford, CA, 94305 USA
[2]Molecular Genetic Pathology Laboratory, Stanford Health Care, Stanford, CA, 94305 USA
[3]Department of Genetics, Stanford University School of Medicine, Stanford, CA, 94305 USA
[4]Department of Biomedical Data Science, Stanford University School of Medicine, Stanford, CA, 94305 USA
*Correspondence to: Helio A. Costa, Ph.D. (H.A.C.), Stanford University, Department of Pathology, 300 Pasteur Drive, MSOB x313, Stanford, CA 94305. Email: hcosta@stanford.edu.

Number of text pages: 19

Tables: 3

Figures: 2

Sources of support: This research was funded by grants from the National Institutes of Health (ClinGen 4U01HG007436-04 to C.D.B.; NCI 2PO1CA49605 to J.L.Z), and from Stanford University Department of Pathology to H.A.C.

Disclosure: C.D.B. is on the scientific advisory boards (SAB) of AncestryDNA, Arc Bio LLC, Etalon DX, Liberty Biosecurity, and Personalis. C.D.B. is on the board of EdenRoc Sciences LLC. C.D.B. is also a founder and SAB chair of ARCBio. H.A.C. provides consulting services to Gerson Lehrman Group LLC. None of these entities played a role in the design, execution, interpretation, or presentation of this study.

Abstract:

RNA sequencing is emerging as a powerful technique to detect a diverse array of fusions in human neoplasia, but few clinically validated assays have been described to date. We designed and validated a hybrid-capture RNAseq assay for FFPE tissue (Fusion-STAMP). It fully targets the transcript isoforms of 43 genes selected for their known impact as actionable targets of existing and emerging anti-cancer therapies (especially in lung adenocarcinomas), prognostic features, and/or utility as diagnostic cancer biomarkers (especially in sarcomas). 57 fusion results across 34 samples were evaluated. Fusion-STAMP demonstrated high overall accuracy with 98% sensitivity and 94% specificity for fusion detection. There was high intra- and inter-run reproducibility. Detection was sensitive to approximately 10% tumor, though this is expected to be impacted by fusion transcript expression levels, hybrid capture efficiency, and RNA quality. Challenges of clinically validating RNA sequencing for fusion detection include a low average RNA quality in FFPE specimens, and variable RNA total content and expression profile per cell. These challenges contribute to highly variable on-target rates, total read pairs, and total mapped read pairs. False positive results may be caused by intergenic splicing, barcode hopping / index hopping, or misalignment. Despite this, Fusion-STAMP demonstrates high overall performance metrics for qualitative fusion detection and is expected to provide clinical utility in identifying actionable fusions.

Keywords: RNAseq; FFPE; Tumor Genotyping; Structural Variation; Chromosomal Fusions

Introduction:

In human neoplasia, numerous clinically relevant translocations have been described, and more continue to be identified. Many are specific to one or several diagnoses, especially among soft tissue neoplasms. In conjunction with clinical history and histomorphologic/immunohistochemical findings, the detection of one of these translocations is a valuable diagnostic adjunct[1]. For example, in the setting of a small round blue cell tumor, translocation testing can help distinguish among differential diagnoses that include Ewing sarcoma, Ewing-like sarcomas, desmoplastic small round cell tumor, alveolar rhabdomyosarcoma, and synovial sarcoma, all of which are associated with distinct translocations or sets of translocations.

Other translocations may guide therapeutic decision making to optimally utilize targeted therapies, particularly in the setting of non-small cell lung carcinoma (NSCLC)[2]. For example, ALK, ROS1, and RET rearrangements are standard-of-care biomarkers predictive of a response to an FDA-approved medication in the setting of NSCLC. In addition, evidence is accumulating for clinical actionability of many other structural rearrangements in NSCLC and other tumors[3–5].

Numerous techniques have been employed to detect fusions[3]. Traditional methods that do not employ next generation sequencing (NGS) include karyotyping, reverse transcriptase polymerase chain reaction (RT-PCR), and fluorescent in situ hybridization (FISH). Each of these methods has specific strengths and limitations. Karyotyping relies on growing cells in culture, can only detect large-scale alterations, demands significant interpretation time and can suffer from long turnaround time. RT-PCR is a sensitive and specific technique to test for well-characterized fusions with stereotyped breakpoints, but suffers from a limited ability to multiplex, or to detect novel rearrangements. FISH is considered the current gold standard for

detecting fusions; though it greatly improves resolution compared to karyotyping, it still suffers from reduced sensitivity compared to NGS-based methods[6], especially for small intrachromosomal events ("cryptic rearrangements"). Furthermore, FISH is unable to determine more granular details pertaining to fusions, including the fusion breakpoints, involved exons, and whether the fusion is in-frame or not. There is emerging evidence that these parameters may be clinically relevant. For example, in one reported cohort of patients with NSCLC positive by FISH testing for an EML4-ALK rearrangement and treated with ALK inhibitors, upon DNA and RNA NGS sequencing, patients with a predicted non-productive or no NGS-detectable EML4-ALK fusion demonstrated significantly worse mean survival compared to those with a predicted productive rearrangement[7].

In more recent years, NGS-based fusion detection techniques have been developed. These include genomic DNA sequencing with target enrichment for regions in which breakpoints occur (such as selected "hotspot" introns)[8,9], whole-transcriptome RNA sequencing utilizing poly(A) capture[10], and targeted RNA sequencing employing hybridization-based capture[11,12] or anchored multiplex PCR[13]. Broadly speaking, NGS-based techniques offer the advantage of greater breadth, depth, and resolution compared to traditional methods, with a tradeoff of increased cost.

Fresh tissue offers the best biospecimen quality characteristics for most molecular assays, but suffers from a lack of convenience, availability, and portability. In both clinical and research settings, formalin-fixed paraffin-embedded (FFPE) tissue has key advantages. These include being generated routinely in the clinical workflow and being a stable source of DNA and/or RNA for years after the tissue is acquired from the patient. In clinical practice, the need for fusion detection may not become apparent until after specimens are fixed and sections are

104 examined under the microscope by a pathologist; also, the clinical need for fusion detection may
105 change over time due to changes in the patient's disease status, or evolution of knowledge in the
106 field. However, FFPE presents significant biospecimen quality challenges to molecular assays
107 due to chemical modifications including cross-linking which occur to DNA and RNA during
108 fixation[14,15]. Cross-linking results in fragmentation, which limits the quantity of intact nucleic
109 acids available for testing, and the obtainable length of NGS sequencing reads.

110 Each NGS-based fusion detection technique has advantages and limitations. Targeted
111 DNA panels commonly used in cancer profiling can conveniently incorporate fusion detection by
112 covering "hotspot" breakpoint regions and detecting fusion "spanning" or fusion "straddling"
113 reads[8,9]. However, these panels can only capture a fraction of possible breakpoints, limited by
114 intron sizes and fusion breakpoint diversity. Furthermore, targeted DNA panels on FFPE
115 specimens have difficulties with repetitive or low complexity regions due to short read lengths;
116 unfortunately, such regions often mediate genomic rearrangements[16]. On the other hand, RNA-
117 based methods cannot detect rearrangements that do not lead to a fusion transcript, such as those
118 that upregulate a gene's expression by juxtaposing an enhancer element (eg, rearrangements
119 involving IGH in some types of lymphoma), and may also miss lowly-expressed fusion
120 transcripts. However, RNA-based NGS techniques can efficiently detect a diverse range of
121 fusion breakpoints. Whole-transcriptome RNA sequencing using poly(A) capture on FFPE
122 specimens for fusion detection has recently been reported[10]. This approach offers a wide breadth
123 of sequencing and correspondingly a high discovery potential for novel fusions, which may be
124 especially valuable in a research setting. However, due to RNA fragmentation, sensitivity
125 decreases with the distance of the breakpoint from the poly(A) tail (ie breakpoints that are more
126 5' in the fusion transcript suffer from reduced sensitivity)[10]. In addition, increased breadth of

sequencing results in detection of more fusions of uncertain clinical significance. Some such fusions may be relevant but not yet understood, while others are likely to be "passenger fusions" which are not driving the cancer, but instead relate to copy number alterations or other structural alterations in cancers with genomic instability[17]. Whole-transcriptome sequencing also suffers from high cost and a prolonged turnaround time.

Currently, genes in which fusions are known to have clinical relevance comprise a small subset of the exome. A targeted panel enables optimization for cost-effective and sensitive detection of clinically relevant alterations. We have validated the Stanford Tumor Actionable Mutation Panel for Fusions (Fusion STAMP), a hybrid-capture based RNAseq assay (run on the Illumina MiSeq) that fully targets the transcript isoforms of 43 genes selected on the basis of their known impact as actionable targets of existing and emerging anti-cancer therapies, their prognostic features, and/or their utility as diagnostic cancer biomarkers. The targeted sequencing approach and integrated bioinformatics workflow is optimized for sequencing of FFPE tumor tissue specimens. In total, 34 unique samples (31 patient specimens, 1 purified RNA reference standard, and 2 RNA-FFPE reference standards [Horizon Discovery]) were tested in parallel by the Fusion STAMP method and compared to other reference methods to assess accuracy, yielding 57 fusion results. Reference methods included our in-house validated NGS panel for solid tumors (Stanford Actionable Mutation Panel; STAMP), validated fluorescence in situ hybridization (FISH) assays, and external reference testing performed by College of American Pathologists (CAP)-accredited laboratories. Analytical specificity was assessed using six non-neoplastic FFPE samples. Analytical sensitivity was assessed through serial dilution of an EWSR1 fusion cell line and by multiple analyses of the Seraseq Fusion RNA Mix v3 (SeraCare 0710-0431) which includes certified quantification of transcript levels by digital PCR. Intra-run,

inter-run, and inter-instrument reproducibility was assessed. Here we describe the validation and anticipated clinical utility of Fusion STAMP.

Materials and Methods:

Specimens and nucleic acid extraction

The patient tissue specimens described in this study were obtained from FFPE tissue blocks from Stanford Health Care. An anatomical pathologist reviewed, diagnosed, and estimated tumor purity from hematoxylin and eosin (H&E) slides of each specimen. A reference purified RNA sample (Seraseq Fusion RNA Mix v3; SeraCare, Cat. No. 0710-0431, Milford, MA, USA) harboring 14 known fusions targeted by our Fusion-STAMP panel was used as a positive control for our analyses. A reference FFPE sample with five fusion transcripts (EML4-ALK, CCDC6-RET, SLC34A2-ROS1, TPM3-NTRK1 and ETV6-NTRK3) confirmed to be present by endpoint RT-PCR (5-Fusion Multiplex (Positive Control) FFPE RNA Reference Standard; Horizon Discovery, Cat. No. HD796, Cambridge, UK) and a reference FFPE sample with the same five fusion transcripts confirmed to be absent by endpoint RT-PCR (5-Fusion Multiplex (Negative Control) FFPE RNA Reference Standard; Horizon Discovery, Cat. No. HD783, Cambridge, UK) were also tested. For dilution studies, a cell line containing an EWSR1 fusion (RD-ES (ATCC® HTB-166™); American Type Culture Collection (ATCC), Manassas, VA, USA) and a B-lymphocyte cell line from a patient with cystic fibrosis (GM07469; Coriell Institute for Medical Research, Camden, NJ, USA) were used. Total RNA from patient and control samples were extracted using a Qiagen RNeasy FFPE Kit (Qiagen Inc., Cat. No. 73504, Germantown, MD, USA), respectively. Additional specimen details can be found in **Table 2**.

Fusion-STAMP sequencing sample preparation, sequencing, and fusion detection

Total RNA (200ng input) from each specimen underwent cDNA synthesis and construction of sequencing libraries using a KAPA Stranded RNA-Seq Library Preparation Kit (Roche Sequencing, Cat. No. 07277261001, Pleasanton, CA, USA). Five to six samples at a time were then multiplexed and underwent enrichment for a 43-gene targeted RNA fusion panel (Table 1) using Roche SeqCap RNA Choice target enrichment probes spanning the entirety of the gene transcripts of interest (Roche Sequencing, Cat. No. 6953247001, Pleasanton, CA, USA). Sequencing was then performed on an Illumina MiSeq instrument producing 150bp paired end reads. In brief, sequencing reads were mapped to the human reference genome (GRCh38.p12) using the STAR-Fusion algorithm (v 1.1.0). STAR-Fusion uses the STAR aligner[18] to map reads and identify candidate fusion transcripts, which are then processed by the STAR-Fusion algorithm to map junction reads and spanning reads to a reference annotation set and to produce a final fusion transcript list. STAR-Fusion is run with the following parameters: STAR-Fusion_v1.1.0/STAR-Fusion --left_fq <R1.fastq.gz> --right_fq <R2.fastq.gz> --genome_lib_dir <genome reference directory> --FusionInspector validate --annotate examine_coding_effect --extract_fusion_reads. Called variants were annotated for a series of functional predictions using publicly available database annotations via internal perl scripts.

Fluorescent In Situ hybridization (FISH)

FISH analysis was performed on interphase nuclei or metaphase chromosomes with the corresponding break-apart FISH probe as previously described[19].

Statistical analyses

All statistical analyses were performed in the R programming language.

Results:

Overview of Gene Panel Targets

Forty-three genes were targeted by Fusion STAMP based on literature review of clinical utility. Of these, 15 are protein kinases involved in fusions with established or emerging evidence for clinical actionability with targeted therapies[3]; 31 are involved in fusions with diagnostic utility; and 9 are involved in fusions with prognostic utility (Table 1). Some targeted genes are involved in fusions with multiple domains of clinical utility. For example, PAX3-FOXO1 and PAX7-FOXO1 are diagnostic for alveolar rhabdomyosarcoma, and also portend a worse prognosis (especially PAX3-FOXO1) compared to embryonal rhabdomyosarcoma and fusion-negative alveolar rhabdomyosarcoma[20]. Some fusions have differing clinical significance depending on the tumor type and the translocation partner; for example, NTRK3 fusions occur across many solid tumor types and may predict response to targeted therapies including larotrectinib and entrectinib[3], but ETV6-NTRK3 fusions are diagnostic markers for infantile fibrosarcoma, congenital mesoblastic nephroma, and secretory carcinoma of the breast and salivary gland. Overall the selected genes provide clinical utility across multiple scenarios. These include NSCLC, particularly those negative for a typical MAPK pathway driver mutation; sarcomas, especially small round blue cell tumors, or others that are difficult to classify; and select head and neck entities, including certain thyroid and salivary gland tumors.

Overview of Experimental and Computational Workflow

The Fusion STAMP workflow includes isolation of total RNA molecules, followed by efficient preparation of sequencing libraries and a target enrichment approach to capture mRNA transcript regions of interest for sequencing. The enrichment is done using custom designed libraries of capture oligonucleotides that target a specific set of expressed genomic regions. This panel fully targets the major canonical transcript isoforms of the 43 genes described above. The bioinformatic pipeline includes sequencing quality control, paired-end mapping to the human transcriptome, and detection of gene fusion events using the STAR-Fusion algorithm. In addition, quality control metrics and plots are generated from the aligned BAM files. A molecular genetic pathology fellow or clinical molecular genetics fellow reviews all fusion variant calls.

Sequencing Metrics and Clinical Reporting Thresholds

Sequencing metrics across the 34 tested samples (Table 2) demonstrate significant variability in on-target rate (range: 28.6 - 93.0%), total read pairs (range: 539,759 – 11,242,774), mapped read pairs (range: 298,880 – 8,530,449), and insert size (range: 144 – 269 bp) despite uniform input RNA mass (200 ng) for all specimens.

True positive fusions had variable read support in the validation cohort, sometimes <20 junction reads (i.e. a read that aligns as a split read at the site of the putative fusion junction). Also, in many samples, low numbers of junction reads (generally <20) were identified for fusions which did not fit in the clinical or biological context, and had not been previously reported in the literature. These were often adjacent or nearby in the genome (possibly representing intergenic splicing[21]). Based on the levels of junction read support for true positive fusions and this presumed noise in the validation data, clinical reporting thresholds were set to

optimize performance metrics in the validation cohort. A "whitelist" was created of fusions which have previously been reported in the literature, and a lower reporting threshold was set for these fusions. A higher threshold was set for fusions with identical breakpoints to one or more other multiplexed samples, due to the phenomenon of barcode hopping[22]. For clinical testing, fusions with supporting junction reads below the reporting threshold that are suspected of being diagnostically or clinically significant may be confirmed by RT-PCR and Sanger sequencing, or by another corroborating result (such as FISH).

Analytical Sensitivity / Limit of Detection, and Analytical Specificity

Analytical sensitivity was assessed with six replicates of the Seraseq Fusion RNA Mix v3, which contains 14 fusion variants whose presence is confirmed and quantitated by digital PCR. Supporting junction reads for 13 of the 14 fusions were detected in all replicates. There was not a clear proportional relationship between the ddPCR copy number as reported by SeraCare (which is based on the number of supportive reads with unique start sites), and the number of supporting junction reads detected on Fusion STAMP. One fusion (TMPRSS2-ERG) was not detected in one replicate (1/6; 17%), and junction read support for this fusion was low in the other replicates. Since this fusion appeared to be near the limit of detection of the Fusion STAMP assay, detection of this fusion was dropped from QC requirements for clinical testing.

Limit of detection was further assessed with a cell line dilution study. Single-replicate serial dilutions were performed using a cell line with an EWSR1 fusion, and a cystic fibrosis cell line (Figure 2). Junction read support of $\geq$20 reads was demonstrated down to a dilution of 6.25%. Of note, 3 junction reads were detected in the 100% cystic fibrosis cell line sample. This is below the established reporting threshold and may suggest barcode hopping or trace

contamination. Overall, based on this data, the sensitivity of Fusion STAMP is cited as approximately 10% tumor.

Analytical specificity was assessed by testing 6 non-neoplastic tissue FFPE specimens. No fusions were detected above the reporting threshold in these samples.

Reproducibility (Precision)

Intra-run and inter-run reproducibility were assessed in three replicates each of the Seraseq Fusion RNA Mix v3 and two clinical samples, one with an EML4-ALK translocation, and the other with a MYO5C-ROS1 translocation. All fusions in the Seraseq control (excluding the TMPRSS2-ERG fusion), and the EML4-ALK and MYO5C-ROS1 fusions, were detected across all replicates.

Accuracy

Fusion STAMP showed excellent accuracy (Table 3). One case was negative by FISH for USP6 but Fusion STAMP was positive for a COL1A1-USP6 fusion. Given the tumor context (a fibro-osseous pseudotumor of the digit), this likely represents a false negative result by FISH testing. Fusion-STAMP is expected to show greater analytical sensitivity than FISH.

One case was positive by outside testing for an EML4-ALK rearrangement, but this was not detected by Fusion STAMP. In this case, the outside lab performed micro-dissection for tumor enrichment. This was not an option with the material received for Fusion STAMP; this may account for this false negative result.

Of the 43 genes in this panel, 27 are involved in at least one fusion in the validation data set. Of the remaining 16 genes, many are rarely involved in fusions, making it a challenge to

obtain reference material. To demonstrate that the selector was successful in capturing these transcripts when expressed, we examined the coverage data in appropriate tissue types among our validation samples. Demonstrable capture was identified for all transcripts on the selector in at least one sample.

Discussion:

Though RNAseq on FFPE promises multiple advantages over DNA sequencing, it also comes with numerous challenges. This includes a low average RNA quality in FFPE specimens, and variable RNA total content and expression profile per cell. The downstream effects of these issues can be seen in highly variable on-target rates, total read pairs, and total mapped read pairs in the Fusion STAMP validation cohort. Tumor percentage estimates, while still important, are less directly related to the fraction of RNA read pairs that originate from the tumor than they would be for DNA. It is conceivable that a lowly expressed fusion could be missed despite relatively high tumor percentage, especially in a poor-quality specimen. Also, given the multiplex design, even though the hybrid capture input RNA mass per sample is constant, variable expression profiles between samples can result in disproportionate sequencing of some samples with greater RNA content aligning to the selector at the expense of other samples.

The sensitivity of Fusion STAMP is estimated to be around 10% tumor based on the EWSR1 cell line dilution study performed during validation; however, this sensitivity is expected to vary significantly by the hybrid capture efficiency of the involved genes, the fusion transcript expression level, and the specimen quality. One false negative was identified in the validation cohort and appears likely to relate to low tumor percent due to lack of enrichment, and

poor RNA quality. However, Fusion STAMP demonstrated high sensitivity for fusion detection overall.

False positive results may be caused by intergenic splicing[21], barcode hopping / index hopping[22], or misalignment. These findings are expected to vary depending on the expression profile of the sample, and therefore will likely vary by the site of origin of the tissue. The full range of human tissue types is near-impossible to comprehensively assess during validation. Several tissue types were tested during validation including lung, gastrointestinal tract, and soft tissue, and no false positives were detected above the reporting thresholds. As clinical testing continues and more tissue types are sequenced, recurrent artifacts will be prospectively tracked, identified, and/or filtered.

Multiple RNA NGS sequencing quality control strategies and metrics have been described in the literature. These include spike-in control transcripts and corresponding probes to assess efficiency of hybrid capture and indirectly assess RNA quality[11]; probes to RNA from housekeeping genes to assess RNA quality[11]; a minimum total mapped read count[10,11,13]; a minimum on-target rate[11]; a minimum mapped exon-exon junction read count[10]; a percent of mapped reads that map to coding regions[10]; and qPCR-based assessment of RNA quality[13]. The utility of these metrics needs to be weighed against the theoretical possibility of detecting a highly expressed fusion despite poor quality, or of missing a lowly expressed fusion despite high quality. This makes it challenging to have an accurate assessment of the risk of a false positive or negative result in any individual case. For this Fusion STAMP validation cohort, despite employing only run-level QC criteria and sample-specific total mapped reads QC cutoffs, after optimizing reporting cutoffs to exclude noise and include real events as confirmed by ancillary

testing, the cohort demonstrates a high sensitivity, specificity, precision and accuracy for qualitative fusion detection.

Conclusions:

Fusion STAMP is a hybrid-capture based RNAseq assay (run on the Illumina MiSeq) that fully targets the transcript isoforms of 43 genes selected on the basis of their known impact as actionable targets of existing and emerging anti-cancer therapies, their prognostic features, and/or their utility as diagnostic cancer biomarkers. Despite challenges related to sequencing RNA from FFPE tissue, after optimizing cutoffs to exclude noise and include real events, this validation cohort demonstrates a high sensitivity, specificity, precision and accuracy for fusion detection. This assay is expected to provide clinical utility in the setting of NSCLC, particularly those negative for any known driver mutation; sarcomas, especially small round blue cell tumors, or others that are difficult to classify; and select head and neck entities, including certain thyroid and salivary gland tumors.

Acknowledgements: All authors contributed to the study design. C.J., S.S., H.Z. and H.A.C. performed the benchwork experiments. E.F. and H.A.C. performed the computational analyses. All authors contributed to the final draft of the manuscript. H.A.C. is the guarantor of this work, and, as such, had full access to all of the data in the study and takes responsibility for the integrity of the data and the accuracy of the data analysis.

References:

1. Fletcher, C. D.M., Bridge, J.A., Hogendoorn, P., Mertens F, editor. WHO Classification of

Tumours of Soft Tissue and Bone. 4th Editio. Lyon, France, International Agency for Research on Cancer, 2013

2. Lindeman NI, Cagle PT, Aisner DL, Arcila ME, Beasley MB, Bernicker EH, Colasacco C, Dacic S, Hirsch FR, Kerr K, Kwiatkowski DJ, Ladanyi M, Nowak JA, Sholl L, Temple-Smolkin R, Solomon B, Souter LH, Thunnissen E, Tsao MS, Ventura CB, Wynes MW, Yatabe Y. Updated molecular testing guideline for the selection of lung cancer patients for treatment with targeted tyrosine kinase inhibitors guideline from the college of American pathologists, the international association for the study of lung cancer, and the association for molecular pathology. Arch. Pathol. Lab. Med., vol. 142, College of American Pathologists, 2018, pp. 321–46

3. Schram AM, Chang MT, Jonsson P, Drilon A. Fusions in solid tumours: Diagnostic strategies, targeted therapy, and acquired resistance. Nat Rev Clin Oncol, 2017, 14:735–48

4. Yoshihara K, Wang Q, Torres-Garcia W, Zheng S, Vegesna R, Kim H, Verhaak RGW. The landscape and therapeutic relevance of cancer-associated transcript fusions. Oncogene, 2015, 34:4845–54

5. Kumar-Sinha C, Kalyana-Sundaram S, Chinnaiyan AM. Landscape of gene fusions in epithelial cancers: Seq and ye shall find. Genome Med, 2015, 7

6. Ali SM, Hensing T, Schrock AB, Allen J, Sanford E, Gowen K, Kulkarni A, He J, Suh JH, Lipson D, Elvin JA, Yelensky R, Chalmers Z, Chmielecki J, Peled N, Klempner SJ, Firozvi K, Frampton GM, Molina JR, Menon S, Brahmer JR, MacMahon H, Nowak J, Ou S-HI, Zauderer M, Ladanyi M, Zakowski M, Fischbach N, Ross JS, Stephens PJ, Miller VA, Wakelee H, Ganesan S, Salgia R. Comprehensive Genomic Profiling Identifies a Subset of Crizotinib-Responsive *ALK* -Rearranged Non-Small Cell Lung Cancer Not

Detected by Fluorescence In Situ Hybridization. Oncologist, 2016, 21:762–70

7. Rosenbaum JN, Bloom R, Forys JT, Hiken J, Armstrong JR, Branson J, McNulty S, Velu PD, Pepin K, Abel H, Cottrell CE, Pfeifer JD, Kulkarni S, Govindan R, Konnick EQ, Lockwood CM, Duncavage EJ. Genomic heterogeneity of ALK fusion breakpoints in non-small-cell lung cancer. Mod Pathol, 2018, 31:791–808

8. Abel HJ, Al-Kateb H, Cottrell CE, Bredemeyer AJ, Pritchard CC, Grossmann AH, Wallander ML, Pfeifer JD, Lockwood CM, Duncavage EJ. Detection of gene rearrangements in targeted clinical next-generation sequencing. J Mol Diagnostics, 2014, 16:405–17

9. Duncavage EJ, Abel HJ, Szankasi P, Kelley TW, Pfeifer JD. Targeted next generation sequencing of clinically significant gene mutations and translocations in leukemia. Mod Pathol, 2012, 25:795–804

10. Winters JL, Davila JI, McDonald AM, Nair AA, Fadra N, Wehrs RN, Thomas BC, Balcom JR, Jin L, Wu X, Voss JS, Klee EW, Oliver GR, Graham RP, Neff JL, Rumilla KM, Aypar U, Kipp BR, Jenkins RB, Jen J, Halling KC. Development and Verification of an RNA Sequencing (RNA-Seq) Assay for the Detection of Gene Fusions in Tumors. J Mol Diagnostics, 2018, 20:495–511

11. Reeser JW, Martin D, Miya J, Kautto EA, Lyon E, Zhu E, Wing MR, Smith A, Reeder M, Samorodnitsky E, Parks H, Naik KR, Gozgit J, Nowacki N, Davies KD, Varella-Garcia M, Yu L, Freud AG, Coleman J, Aisner DL, Roychowdhury S. Validation of a Targeted RNA Sequencing Assay for Kinase Fusion Detection in Solid Tumors. J Mol Diagnostics, 2017, 19:682–96

12. Cieslik M, Chugh R, Wu YM, Wu M, Brennan C, Lonigro R, Su F, Wang R, Siddiqui J,

Mehra R, Cao X, Lucas D, Chinnaiyan AM, Robinson D. The use of exome capture RNA-seq for highly degraded RNA with application to clinical cancer sequencing. Genome Res, 2015, 25:1372–81

13. Zhu G, Benayed R, Ho C, Mullaney K, Sukhadia P, Rios K, Berry R, Rubin BP, Nafa K, Wang L, Klimstra DS, Ladanyi M, Hameed MR. Diagnosis of known sarcoma fusions and novel fusion partners by targeted RNA sequencing with identification of a recurrent ACTB-FOSB fusion in pseudomyogenic hemangioendothelioma. Mod Pathol, 2018. https://doi.org/10.1038/s41379-018-0175-7

14. Wang F, Wang L, Briggs C, Sicinska E, Gaston SM, Mamon H, Kulke MH, Zamponi R, Loda M, Maher E, Ogino S, Fuschs CS, Li J, Hader C, Makrigiorgos GM. DNA degradation test predicts success in whole-genome amplification from diverse clinical samples. J Mol Diagnostics, 2007, 9:441–51

15. Srinivasan M, Sedmak D, Jewell S. Review Effect of Fixatives and Tissue Processing on the Content and Integrity of Nucleic Acids. vol. 161. 2002

16. Lawson ARJ, Hindley GFL, Forshew T, Tatevossian RG, Jamie GA, Kelly GP, Neale GA, Ma J, Jones TA, Ellison DW, Sheer D. RAF gene fusion breakpoints in pediatric brain tumors are characterized by significant enrichment of sequence microhomology. Genome Res, 2011, 21:505–14

17. Kalyana-Sundaram S, Shankar S, DeRoo S, Iyer MK, Palanisamy N, Chinnaiyan AM, Kumar-Sinha C. Gene Fusions Associated with Recurrent Amplicons Represent a Class of Passenger Aberrations in Breast Cancer. Neoplasia, 2015, 14:702-IN13

18. Dobin A, Davis CA, Schlesinger F, Drenkow J, Zaleski C, Jha S, Batut P, Chaisson M, Gingeras TR. STAR: Ultrafast universal RNA-seq aligner. Bioinformatics, 2013, 29:15–

21

19. Nybakken GE, Bala R, Gratzinger D, et al. Isolated Follicles Enriched for Centroblasts and Lacking t(14;18)/BCL2 in Lymphoid Tissue: Diagnostic and Clinical Implications. Pagano JS, ed. *PLoS ONE*. 2016;11(3):e0151735. doi:10.1371/journal.pone.0151735.

20. Missiaglia E, Williamson D, Chisholm J, Wirapati P, Pierron G, Petel F, Concordet JP, Thway K, Oberlin O, Pritchard-Jones K, Delattre O, Delorenzi M, Shipley J. PAX3/FOXO1 fusion gene status is the key prognostic molecular marker in rhabdomyosarcoma and significantly improves current risk stratification. J Clin Oncol, 2012, 30:1670–7

21. Jividen K, Li H. Chimeric RNAs generated by intergenic splicing in normal and cancer cells. Genes Chromosom Cancer, 2014, 53:963–71

22. Illumina. Effects of Index Misassignment on Multiplexing and Downstream Analysis. Illumina, 2017:1–4

447

448

449

450

451

452

453 **Table 1**: Fusion-STAMP gene panel with affiliated cancer(s) and clinical utility.

Gene	Cannonical RefSeq Transcript (length in bp)	Translocation or Other Alteration	Affiliated Cancer(s)	Clinical Utility	Actionable Therapy
ALK	NM_004304.4 (6267)	EML4-ALK and others	Non-small cell lung carcinoma	Predictive	FDA Approved: Crizotinib, Brigatinib, Alectinib, Ceritinib Under Investigation: Lorlatinib, Entrectinib, Belizatinib, Ensartinib CEP-37440
			Inflammatory myofibroblastic tumor	Diagnostic Predictive	Standard of Care: Crizotinib, Ceritinib
		NPM1-ALK	ALK+ anaplastic large cell lymphoma	Diagnostic Predictive	Under Investigation: ALK inhibitors
ROS1	NM_002944.2 (7368)	ROS1 fusions	Non-small cell lung carcinoma	Predictive	FDA Approved: Crizotinib Under Investigation: Entrectinib, Ceritinib
MET	NM_000245.2 (6641)	MET fusions	Gliomas	Predictive	--
RET	NM_020975.4 (5629)	RET fusions	Non-small cell lung carcinoma	Predictive	FDA Breakthrough: LOXO-292 Standard of Care: Cabozantinib, Vandetanib Under Investigation: Lenvatinib, Ponatinib, Sunitinib, Sorafenib, Apatinib
EGFR	NM_005228.3 (5616)	EGFR fusions	Non-small cell lung carcinoma	Predictive	Under Investigation: Erlotinib
NRG1	NM_013964.3 (3078)	NRG1 fusions	Non-small cell lung carcinoma	Predictive	Under Investigation: Afatinib

RAF1 (CRAF)	NM_002880.3 (3291)	RAF1 fusions	Multiple solid tumor types	Predictive	Under Investigation: LXH254, LY3009120, MEK inhibitors
BRAF	NM_004333.4 (2949)	BRAF fusions	Melanoma	Predictive	Under Investigation: Second-generation BRAF inhibitors (PLX7904, PLX8394, LXH254), MEI inhibitors (Cobimetinib, Trametinib)
			Ovarian cancer		
			Other solid tumors	Predictive	
COL1A1	NM_000088.3 (5927)	COL1A1-PDGFB	Dermatofibrosarcoma protruberans	Diagnostic Predictive	Under Investigation: Imatinib
PDGFB	NM_002608.3 (3801)				
FGFR1	NM_023110.2 (5917)	FGFR1, FGFR2, and FGFR3 fusions	Multiple solid tumor types	Predictive	Under Investigation: AZD4547, Erdafitinib, BGJ398, Debio1347, Infigratinib, ARQ-087
FGFR2	NM_000141.4 (4654)				
FGFR3	NM_000142.4 (4304)				
NTRK1	NM_002529.3 (2663)	NTRK1, NTRK2, and NTRK3 fusions	Multiple solid tumor types	Predictive	FDA Approved: Larotrectinib Under Investigation: Entrectinib
NTRK2	NM_001018064.2 (8498)				
NTRK3	NM_001012338.2 (3004)				
		ETV6-NTRK3	Infantile fibrosarcoma	Diagnostic	--
ETV6	NM_001987.4 (5989)		Congenital mesoblastic nephroma	Diagnostic	--
			Secretory carcinoma of breast and of salivary gland	Diagnostic	--
BCOR	NM_001123385.1 (6434)	BCOR-CCNB3	Ewing-like sarcoma, BCOR-rearranged	Diagnostic Prognostic (similar to Ewing sarcoma)	--
CCNB3	NM_033031.2 (4524)				
CIC	NM_001304815.1 (8245)	CIC-DUX4	Ewing-like sarcoma, CIC-rearranged	Diagnostic Prognostic (worse than Ewing sarcoma)	
CAMTA1	NM_015215.3 (8444)	WWTR1-CAMTA1	Epithelioid hemangioendothelioma	Diagnostic	--
ERG	NM_001136154.1 (5114)	TMPRSS2-ERG	Ewing sarcoma	Diagnostic	--
DDIT3	NM_004083.5 (924)	FUS-DDIT3, EWSR1-DDIT3	Myxoid liposarcoma	Diagnostic	--
FUS	NM_004960.3				

	(5119)	FUS-CREB3L2	Low grade fibromyxoid sarcoma	Diagnostic	--
		FUS-ATF1	Angiomatoid fibrous histiocytoma	Diagnostic	--
ATF1	NM_005171.4 (2505)				
		EWSR1-ATF1	Clear cell sarcoma	Diagnostic	--
			Angiomatoid fibrous histiocytoma	Diagnostic	--
			Hyalinizing clear cell carcinoma of the salivary gland	Diagnostic	--
EWSR1, FLI1	NM_002017.4 (3995)	EWSR1-FLI1	Ewing sarcoma	Diagnostic	--
		EWSR1-DDIT3	Myxoid liposarcoma	Diagnostic	--
		EWSR1-NR4A3	Extraskeletal myxoid chondrosarcoma	Diagnostic	--
		EWSR1-CREB1	Angiomatoid fibrous histiocytoma	Diagnostic	--
			Primary pulmonary myxoid sarcoma	Diagnostic	--
		EWSR1-WT1	Desmoplastic small round cell tumor	Diagnostic	--
WT1	NM_024426.4 (3037)				--
PAX3	NM_181457.3 (2032)	PAX3-FOXO1, PAX7-FOXO1	Alveolar rhabdomyosarcoma	Diagnostic Prognostic (adverse)	--
PAX7	NM_001135254.1 (6053)				
FOXO1	NM_002015.3 (5738)				
NAB2	NM_005967.3 (2725)	NAB2-STAT6	Solitary fibrous tumor	Diagnostic	--
STAT6	NM_001178078.1 (4050)				
NCOA2	NM_006540.2 (6157)	HEY1-NCOA2	Mesenchymal chondrosarcoma	Diagnostic	--
PHF1	NM_024165.2 (2312)	EP400-PHF1	Ossifying fibromyxoid tumor	Diagnostic	--
SSX1	NM_001278691.1 (1402)	SSX2-SS18, SSX1-SS18	Synovial sarcoma	Diagnostic	--
SS18	NM_001007559.2 (3440)				
TFE3	NM_006521.5 (3467)	ASPL-TFE3	Translocation carcinoma of kidney	Diagnostic Prognostic (adverse)	--
			Alveolar soft parts sarcoma	Diagnostic	--
USP6	NM_004505.3 (7993)	CDH11-USP6 and others	Aneurysmal bone cyst	Diagnostic	--
		MYH9-USP6 and others	Nodular fasciitis	Diagnostic	--

HMGA2	NM_003483.4 (4150)	HMGA2 fusions	Pleomorphic adenoma	Diagnostic	--
			Carcinoma ex pleomorphic adenoma	Diagnostic	--
MYB	NM_005375.3 (3315)	MYB-NFIB	Adenoid cystic carcinoma	Diagnostic	--
PPARG	NM_015869.4 (1820)	PAX8-PPARG	Follicular thyroid carcinoma	Diagnostic Prognostic (favorable)	--
			Follicular variant of papillary thyroid carcinoma	Diagnostic	--
			Follicular adenoma	Diagnostic	--
YWHAE	NM_006761.4 (1827)	YWHAE-FAM22	Endometrial stromal sarcoma, high grade	Diagnostic Prognostic (adverse)	--

471

472

473

474

475 **Table 2**: Sample pathological and sequencing metrics from Fusion-STAMP validation data. Abbreviations: FISH, fluorescent in situ
476 hybridization; FFPE, formalin fixed paraffin embedded; STAMP, Stanford Actionable Mutation Panel; IHC, immunohistochemistry;
477 AMP, anchored multiplex PCR; NGS, next generation sequencing; ddPCR, digital droplet polymerase chain reaction.

Sample Number	Diagnosis	Tissue Type	Tumor Percentage (%)	On-Target Rate (%)	Total Read Pairs	Total Mapped Read Pairs	Median Insert Size (bp)	Reference Method	Fusion(s) Detected by Fusion-STAMP	Result
1	Adenoid cystic carcinoma	FFPE	Unknown	82.4	6,091,887	4,033,771	194	FISH (MYB)	EWSR1-MYB	TP
2	Round cell liposarcoma	FFPE	Unknown	73.6	3,361,055	2,573,249	231	FISH (FUS)	DDIT3-FUS	TP
3	Inflammatory myofibroblastic tumor	FFPE	20	86.5	5,790,815	4,211,070	251	FISH (ALK)	CLTC-ALK	TP
4	Extraskeletal myxoid chondrosarcoma	FFPE	60	40.1	3,278,632	1,424,224	162	FISH (EWSR1)	EWSR1-NR4A3	TP
5	Synovial sarcoma	FFPE	90	61.0	5,370,991	3,071,753	178	FISH (SS18)	SS18-SSX2	TP
6	Mammary analogue secretory carcinoma	FFPE	30	28.6	2,014,943	520,259	144	FISH (ETV6)	NTRK3-ETV6	TP
7	Angiomatoid fibrous histiocytoma	FFPE	30	87.6	8,811,208	4,679,123	217	FISH (EWSR1)	EWSR1-CREB1	TP
8	Lung adenocarcinoma	FFPE	30	63.8	3,366,719	1,698,839	192	STAMP (EML4-ALK)	EML4-ALK	TP
9	Adenoid cystic carcinoma	FFPE	Unknown	34.5	3,201,447	1,687,063	170	FISH (MYB)	MYB-NFIB	TP
10	Solitary fibrous tumor, malignant	FFPE	80	47.7	4,645,678	2,202,900	154	IHC (STAT6)	NAB2-STAT6	TP
11	Synovial sarcoma	FFPE	80	64.9	5,232,246	3,433,244	193	FISH (SS18)	SS18-SSX2	TP
12	Alveolar soft part	FFPE	60	69.5	5,196,767		201	FISH (TFE3)	ASPSCR1-TFE3	TP

	sarcoma					3,403,879				
13	Lung adenocarcinoma	FFPE	50	52.0	2,357,548	1,171,268	188	STAMP (MYO5C-ROS1)	MYO5C-ROS1	TP
14	Lung adenocarcinoma	FFPE	60	55.0	2,875,396	1,036,438	165	STAMP (KIF5B-RET)	KIF5B-RET	TP
15	Papillary thyroid carcinoma	FFPE	90	76.2	5,101,194	3,094,816	202	STAMP (EML4-ALK)	EML4-ALK	TP
16	Dedifferentiated liposarcoma	FFPE	Unknown	83.9	539,759	298,880	175	External NGS (HMGA2 rearrangement exon 3)	HMGA2-LUM	TP
17	Myeloid neoplasm with eosinophilia	FFPE	Unknown	47.9	3,098,223	1,686,619	165	FISH (FGFR1)	TPR-FGFR1 ZMYM2-FGFR1	TP
18	Pilocytic astrocytoma	FFPE	40	78.5	4,776,729	3,455,673	218	STAMP (KIAA1549-BRAF)	KIAA1549-BRAF	TP
19	Unknown	FFPE	Unknown	75.5	6,199,079	3,117,896	160	External AMP (CCD6-RET)	CCD6-RET	TP
20	Unknown	FFPE	Unknown	84.3	4,334,590	2,612,327	169	External AMP (KIF5B-RET)	KIF5B-RET	TP
21	Fibro-osseous pseudotumor	FFPE	Unknown	73.1	6,610,133	3,589,148	206	External FISH (USP6) - negative	COL1A1-USP6	FP
22	Unknown	FFPE	Unknown	70.5	6,033,595	3,865,529	203	External AMP (MET ex14)	NEGATIVE	TN
23	Unknown	FFPE	Unknown	70.4	6,836,190	3,047,840	167	External AMP (MET ex14)	NEGATIVE	TN
24	Unknown	FFPE	Unknown	75.9	3,197,111	2,041,473	201	External AMP (EML4-ALK)	NEGATIVE	FN
25	Acute myeloid leukemia arising from eosinophilic myeloproliferative	FFPE	4	43.0	2,517,711	624,988	144	STAMP (FIP1L1-PDGFRA)	NEGATIVE	TN

	neoplasm									
26	Clear cell renal cell carcinoma	FFPE	60	85.0	5,738,916	4,291,356	243	STAMP (NEGATIVE)	NEGATIVE	TN
27	Lung adenocarcinoma	FFPE	80	85.0	5,206,099	3,519,763	208	STAMP (NEGATIVE)	NEGATIVE	TN
28	Salivary gland carcinoma	FFPE	30	89.4	1,771,590	1,363,295	210	STAMP (NEGATIVE)	NEGATIVE	TN
29	Lung adenocarcinoma	FFPE	70	84.9	5,168,406	3,845,247	237	STAMP (NEGATIVE)	NEGATIVE	TN
30	Anaplastic oligodendroglioma	FFPE	40	81.9	4,396,856	2,199,939	168	STAMP (NEGATIVE)	NEGATIVE	TN
31	Appendiceal mucinous adenocarcinoma	FFPE	10	93.0	1,124,2774	8,530,449	269	STAMP (NEGATIVE)	NEGATIVE	TN
32	Horizon 5-Fusion Multiplex (Positive Control) FFPE RNA Reference Standard	FFPE	---	69.2	5,206,194	3,800,859	226	Horizon Discovery: positive at 5 certified loci	SLC34A2-ROS1 ETV6-NTRK3 CCD6-RET TPM3-NTRK1 EML4-ALK	TP
33	Horizon 5-Fusion Multiplex (Negative Control) FFPE RNA Reference Standard	FFPE	---	66.7	4,149,750	2,863,989	211	Horizon Discovery: negative at 5 certified loci	NEGATIVE	TN

34	Seraseq Fusion RNA Mix v3	RNA	---	41.7	2,140,929	1,209,775	223	ddPCR (Seraseq)	CD74-ROS1 EGFR-SEPT14 EML4-ALK ETV6-NTRK3 FGFR3-BAIAP2L1 FGFR3-TACC3 KIF5B-RET LMNA-NTRK1 NCOA4-RET PAX8-PPARG1 SLC34A2-ROS1 SLC45A3-BRAF TPM3-NTRK1 TMPRSS2-ERG	TP

Table 3: Table 3: Summary of accuracy testing metrics. Each fusion call, and each negative sample, was counted as one call. Abbreviations: TP, true positive; FP, false positive; FN, false negative; TN, true negative; Sn, sensitivity; Sp, specificity; PPV, positive predictive value; NPV, negative predictive value.

	Fusion-STAMP Positive	Fusion-STAMP Negative	Metric
Reference Method Positive	40 (TP)	1 (FN)	Sn: 98%
Reference Method Negative	1 (FP)	15 (TN)	Sp: 94%

Metric	PPV: 98%	NPV: 94%	Total: 57 calls

482

483

484 **Figure 1**: Fusion-STAMP experimental and computational workflow.

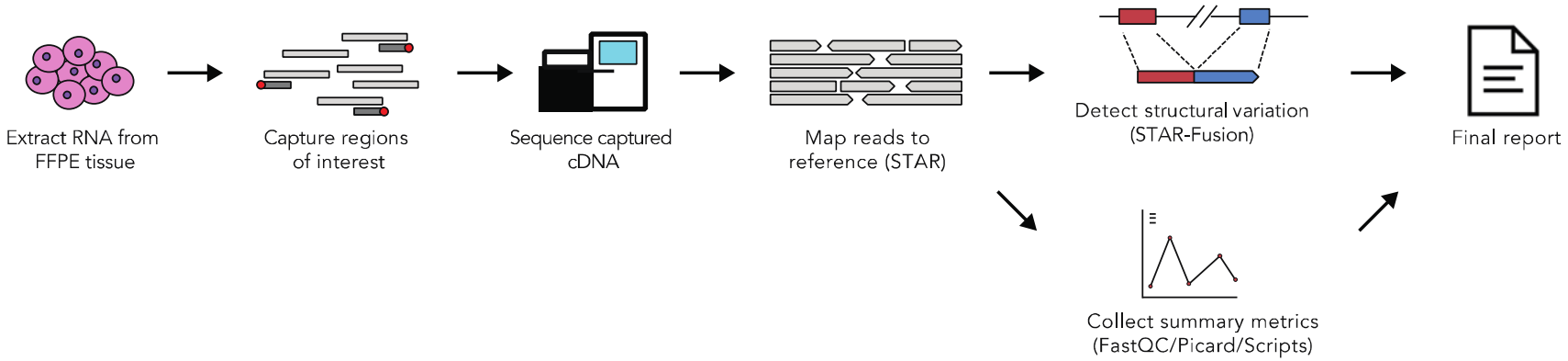

485

486 **Figure 2**: Fusion-STAMP limit of detection study. Single-replicate serial dilutions were performed using a cell line with an EWSR1

487 fusion, and a cystic fibrosis cell line.

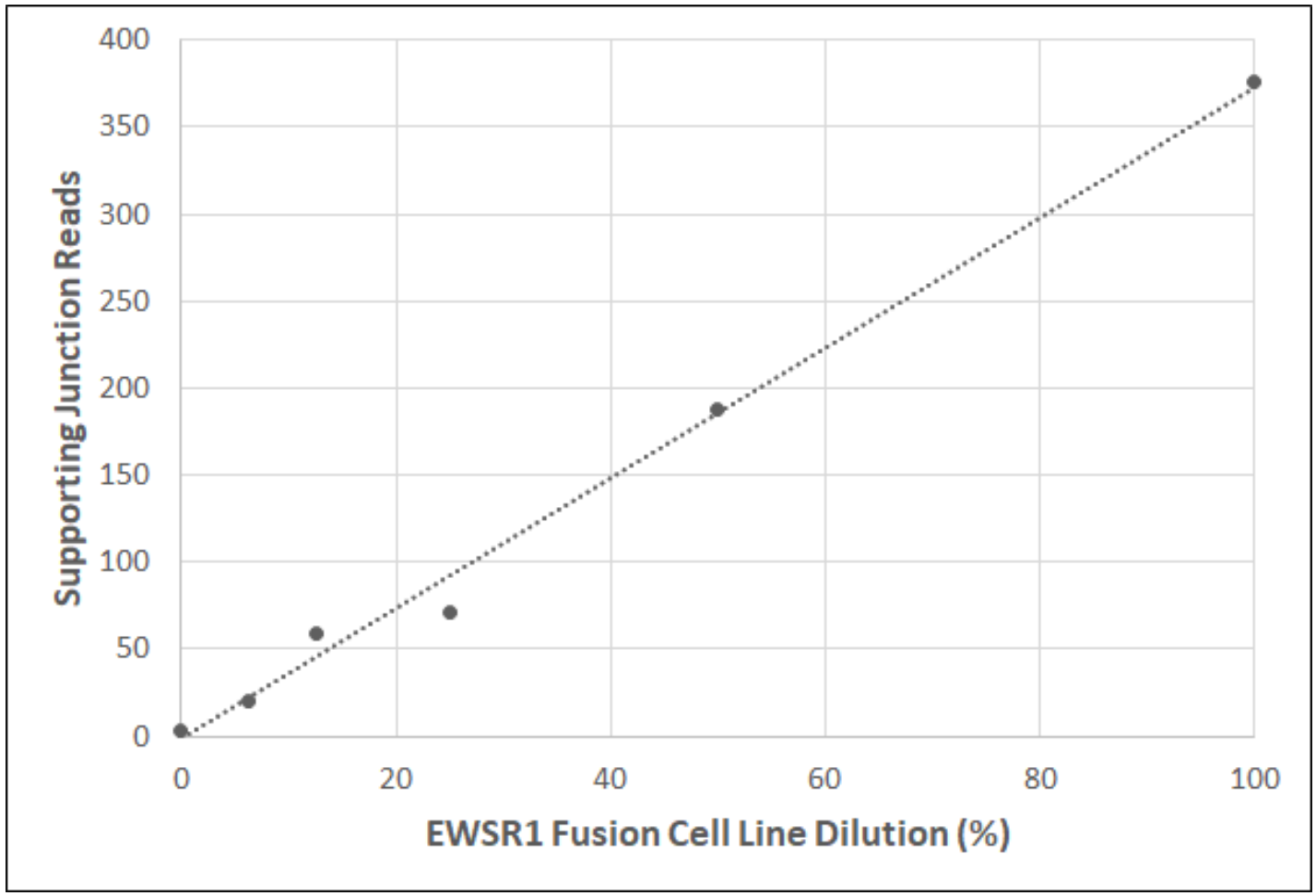

488